Biofouling
Vol. 28, No. 6, July 2012, 551–562

Taylor & Francis
Taylor & Francis Group

Formation of bacterial streamers during filtration in microfluidic systems

Aurélie Marty[a,b], Christine Roques[a,b], Christel Causserand[a,b] and Patrice Bacchin[a,b]*

[a]*Université de Toulouse, INPT, UPS, Laboratoire de Génie Chimique, 118 Route de Narbonne, F-31062 Toulouse, France;* [b]*CNRS, Laboratoire de Génie Chimique, F-31062 Toulouse, France*

(*Received 8 November 2011; final version received 15 May 2012*)

Bacterial behavior during filtration is complex and is influenced by numerous factors. The aim of this paper is to report on experiments designed to make progress in the understanding of bacterial transfer in filters and membranes. Polydimethylsiloxane (PDMS) microsystems were built to allow direct dynamic observation of bacterial transfer across different microchannel geometries mimicking filtration processes. When filtering *Escherichia coli* suspensions in such devices, the bacteria accumulated in the downstream zone of the filter forming long streamers undulating in the flow. Confocal microscopy and 3D reconstruction of streamers showed how the streamers are connected to the filter and how they form in the stream. Streamer development was found to be influenced by the flow configuration and the presence of connections or tortuosity between channels. Experiments showed that streamer formation was greatest in a filtration system composed of staggered arrays of squares 10 μm apart.

Keywords: *Escherichia coli*; filtration; bacterial streamers; micro-channel; biofouling; microseparator

Introduction

In natural and engineered systems, bacteria colonize surfaces and form biofilms. In engineered systems, these biofilms can play a positive role by participating in the removal of organics, for example, in wastewater treatment by a Membrane Bio-Reactor (MBR) (Stephenson et al. 2000; Chu and Li 2005). On the other hand, biofilms can cause health problems as they increase resistance to antimicrobial agents and participate in the transmission of disease. For instance, during the use of membrane processes for drinking water production (Li and Chu 2003), bacterial retention must be maximized while avoiding the formation of an active biofilm on the surface.

The way in which bacteria colonize a porous surface such as a membrane or a filter is not fully known, nor are the conditions that promote the process. Bacterial adhesion and biofilm formation have been shown to be sensitive to numerous biological and physico-chemical factors. The biological factors include the bacterial cell type (Van Loosdrecht et al. 1987; Gannon et al. 1991), their physiology and surface properties (eg the presence of extracellular polymeric substances (EPS)) (Burks et al. 2003; de La Fuente et al. 2007; Ueshima et al. 2008), their motility (de Kerchove and Elimelech 2008), and the surface properties of their cell walls (eg hydrophobicity, surface charge, and the visco-elasticity of the cell envelope) (Schäfer et al. 1998). The chemical properties of aqueous solutions in which the bacteria are dispersed include the ionic strength and pH (Jewett et al. 1995; Abbasnezhad et al. 2008; Torkzaban 2008), which can induce changes in the bacterial wall (Gaboriaud et al. 2008). The physical factors of the fluid include the hydrodynamic conditions, which have been studied with various flow configurations, such as flow chambers (Bruinsma et al. 2001), stagnation points (Redman et al. 2004; Walker et al. 2004) and packed beds (Burks et al. 2003; Redman et al. 2004; Liu and Li 2008).

Depending on these conditions, bacteria can form biofilms with various architectures and microbial activities and the biofilm can form mushroom-like structures on a plane surface but, also, in some cases, filamentous structures called streamers (Stoodley et al. 1998). This kind of biofilm is found between the spacers in nanofiltration and reverse osmosis equipment. The presence of streamers leads to a pressure drop and a decrease in process efficiency (Vrouwenvelder et al. 2009). The behavior of bacteria in a filter or a membrane is affected by this complex interplay between biological and physico-chemical phenomena. Lebleu et al. (2009) have shown that the retention of bacteria in microfiltration membranes is linked to the elasticity of the cell envelope. Moreover, the presence of macropores or membrane defects larger than the bacteria can decrease the retention efficiency, the

*Corresponding author. Email: bacchin@chimie.ups-tlse.fr

ISSN 0892-7014 print/ISSN 1029-2454 online

http://dx.doi.org/10.1080/08927014.2012.695351
http://www.tandfonline.com

bacterial transfer being then monitored by the defect characteristics. There is a need to investigate the transfer of bacteria in conditions similar to those encountered in filtration processes when defects are present. The objective of the work presented here was to develop a filtration system to study the transfer of bacteria through a porous interface and then to determine how bacteria move through the filter and what factors govern their capture. The bacterial species chosen for this study was *Escherichia coli*, which represents a potential source of contamination in water treatment and, as a consequence, is often used to qualify bacterial retention in filtration processes. The microfluidic architecture and the microscopic observation techniques used for this study are presented in the next section. Dynamic microscopy and 3D confocal observations of the formation of streamers are reported. The results and the affect of flow conditions (architecture of the porous zone, flow velocities) were analyzed and interpreted in terms of capture efficiency.

Materials and methods

The experiments were performed with transparent polydimethylsiloxane (PDMS) microfluidic devices that mimic filtration systems. Bacterial suspensions were filtered through these devices. Direct observation by digital video microscopy of bacterial accumulation in micro-channels allowed bacterial capture to be studied while altering the micro-channel geometries, the hydrodynamics and the physico-chemical conditions. Images were then analyzed to quantify the efficiency of the capture of bacteria by the microfiltration system.

Characteristics of the PDMS micro-separator

PDMS micro-separators were designed to mimic filtration in the dead-end mode: one inlet (the feed) and one outlet (the filtrate), or in cross-flow mode: one inlet (the feed) and two outlets (the retentate and the filtrate). In the cross-flow mode experiments, the retentate outlet was closed in order to have the same quantity of bacteria going through the porous zone for both modes and to have the same velocities in the channels, thus it is referred to as the pseudo-cross-flow mode for the remainder of this paper. A sketch of the PDMS dead-end and pseudo-cross-flow filtration micro-separators is shown in Figure 1. The dimensions are detailed in the figure caption. In these systems, the filtering part of the device consisted of a parallel arrangement of 25 micro-channels with a width of 10 μm. Lengths were either 200 μm or 170 μm. Different kinds of micro-channel geometry (straight, interconnected, or staggered) reproduced the various flow conditions that can be encountered during filtration. The depth (along z direction) of all the channels in the network was 50 μm.

These devices were made by the soft lithography technique (McDonald et al. 2000). The PDMS prepolymer and the curing agent (Sylgard 184 silicone elastomer kit, Dow Corning) were mixed in the ratio of 10:1, stirred thoroughly and degassed in a vacuum desiccator. The techniques of PDMS micro-separator preparation and the main surface properties of PDMS are reported in Bacchin et al. (2011).

Bacterial suspension

Escherichia coli strain CIP 54.127 was obtained from the Institute Pasteur collection (Paris, France). Cells

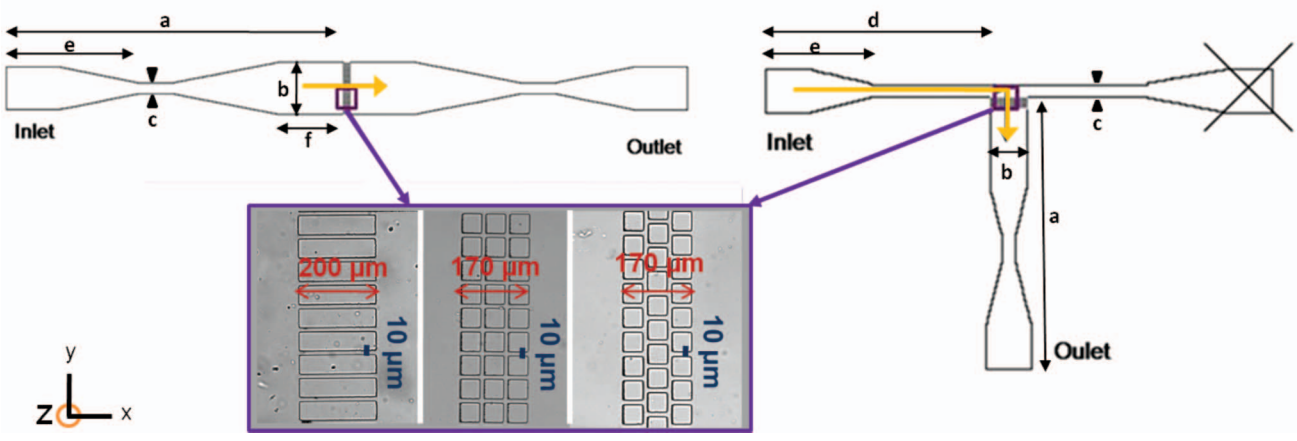

Figure 1. Sketch of the PDMS micro-separators working in the dead-end (left) or pseudo-cross-flow mode (right). The dimensions of the two micro-separators were: a = 12.90 mm; b = 1.70 mm; c = 0.50 mm; d = 11 mm; e = 5 mm; f = 4 mm. The inset details the filtration zone with different micro-channel geometries: straight, connected and staggered (from left to right). Channel widths equal to 5, 10, and 20 μm were used.

were grown aerobically on a complex medium (tryptone soy agar, Biomérieux) and incubated at 37°C for 24 h (stationary phase). For inoculum preparation, isolated colonies were suspended in sterile physiological saline (NaCl 9 g l^{-1}), ie in non-nutritive conditions. The suspension concentration was adjusted to approximately 10^8 cells ml^{-1} by the optical density at 640 nm.

Cell filtration and microscopic observation

The bacterial suspensions were filtered through the PDMS micro-separators with a constant filtration flow rate (1.41 ml h^{-1}) using a syringe pump (PHD 22/2000, Harvard Apparatus). Before filtration, the micro-separators were rinsed with sterile physiological saline. The flows in the micro-channels and in the other zones of the micro-separator were laminar. In a micro-channel, the interstitial velocity was 15.7 mm s^{-1} (Re = 0.45), while in the feed channel, the superficial velocity was 4.53 mm s^{-1} (Re = 0.44) for the dead-end mode and 22.2 mm s^{-1} (Re = 2.01) for the pseudo-cross-flow mode. The characteristic length used for the calculation of the Reynolds number was the hydraulic diameter of the channel. These superficial filtration velocities ($\sim$16 m h^{-1}) are in the range of those used in membrane microfiltration (up to 50 m h^{-1}, based on data for a MF-Millipore membrane with 8 μm pore size, operated at 100 mbar) and in conventional filtration with wooden filters or sand filters (up to 20 m h^{-1} for rapid filtration). The mean residence time in a channel was 13 ms. As shown in Figure 2, the capture of bacteria was followed over 120 min through observation of the micro-channels by an optical microscope (Axiolab, Zeiss). Images were recorded as a movie using a highly light-sensitive camera (Pixelfly QE, PCO) mounted on the microscope with an exposure time of 30 ms (Figure 2) and operated at 2 frames min^{-1}. All experiments were performed a minimum of three times to be sure of the repeatability. The mean standard deviation (SD) was determined at 25 μm and 9.10^{-3} for the average length of streamer and the capture efficiency, respectively. The corresponding confidence intervals at 90% confidence level were $\pm$20 μm and $\pm 6.10^{-3}$ for the average length and the capture efficiency respectively. In the following sections, only one experiment is presented for each condition.

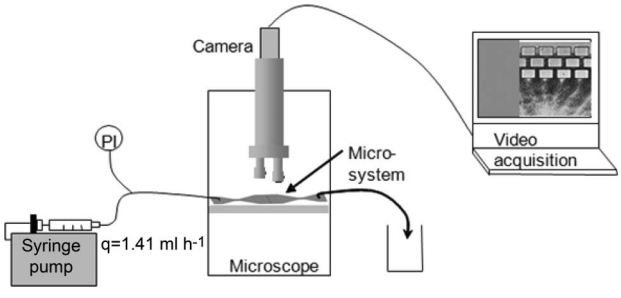

Figure 2. Sketch of the experimental set-up.

Confocal laser scanning microscope (CLSM) observations

The three-dimensional organization of the bacteria was observed by confocal microscopy. Experiments were performed with a confocal microscope (Leica, Heidelberg, Germany) under $\times$10 magnification. Before observing the accumulations, 0.5 ml of the green fluorescing stain Syto9 (5 mM, Molecular Probe, Invitrogen, Eugene, OR, USA) was added directly to the wells. No rinsing was performed before observation because moving bacterial cells were clearly distinguishable from accumulated cells. Concanavalin A (Invitrogen) was introduced into the bacterial suspension to observe the presence of EPS. The 488 nm line of an argon laser was used to excite the emission of Syto9 fluorescence, emitted in the range between 498 and 533 nm. For Concanvalin A, a HeNe 633 nm laser was used and the fluorescence emitted was collected between 642 and 733 nm. Samples were scanned in the xz direction with a step size of 2 μm. Confocal microscopy generated an image stack through the thickness for optical results, marked bacterial results, and marked EPS results. A stack of images was recorded after filtration for 2 h and the streamer reconstructed with AMIRA software.

Image processing

Images obtained with optical microscopy were analyzed to quantify the accumulation of bacteria in the micro-separators. ImageJ software was used to process the stack of images (1360 $\times$ 1024 pixels corresponding to $\sim$1.74 $\times$ 1.31 mm) generated by the video. By using a thresholding technique, the number of pixels corresponding to bacterial accumulation was calculated from the stack. Through calibration of pixel size (783 pixels = 1 mm), it was then possible to determine the microseparator area, A, in mm^2 covered by bacteria. The analysis was performed on the entirety of the observed zone (2.3 mm^2). The data were used to estimate the capture efficiency of bacteria, which corresponds to the ratio of the volume of accumulated bacteria over the volume of bacteria transferred through the microseparator from the beginning of the experiment. The volume of accumulated bacteria was taken to be proportional to the area of accumulated bacteria through the relationship:

$$V = f.A.(1 - \varepsilon) \quad (1)$$

where ε is the porosity of the accumulated bacteria (here, as generally accepted, it is assumed to be 0.38 for random close-packing arrangement) and f is a proportionality factor relative to the way bacteria accumulate in the third direction (ie along the z axis). This last parameter can be affected by two limitations: (a) it is considered that bacteria accumulate in a sheet (forming a surface film in the xy plane one bacterium thick); f is the thickness of one bacterium; (b) it is considered that bacteria accumulate by filling all the space in the third dimension (causing 3D clogging through the whole thickness); f is then the whole thickness of the microseparator (50 μm).

These assumptions correspond to minimal and maximal capture efficiency, respectively. Further investigations by confocal microscopy revealed that bacterial accumulation takes the form of triangular shaped streamers attached across the whole depth of the microsystem, z (as presented later in Figure 5). This observation suggested that bacterial accumulation globally filled half the space available in the microseparators. Therefore, a value of 25 μm was used for f in order to estimate capture efficiency. The capture efficiency is calculated from the following expression:

$$\eta = \frac{V}{Q.C.V_b.t} \tag{2}$$

where V represents the volume (m^3) of bacteria in the streamer calculated by image analysis (defined by Equation (1) and the denominator of the equation is the overall volume of bacteria having flowed through the microseparator. This last term is the product of Q, the flow rate ($m^3\ s^{-1}$), C the bacterial concentration (CFU m^{-3}), V_b the volume of one bacterial cell (m^3 CFU^{-1}) and t the filtration time.

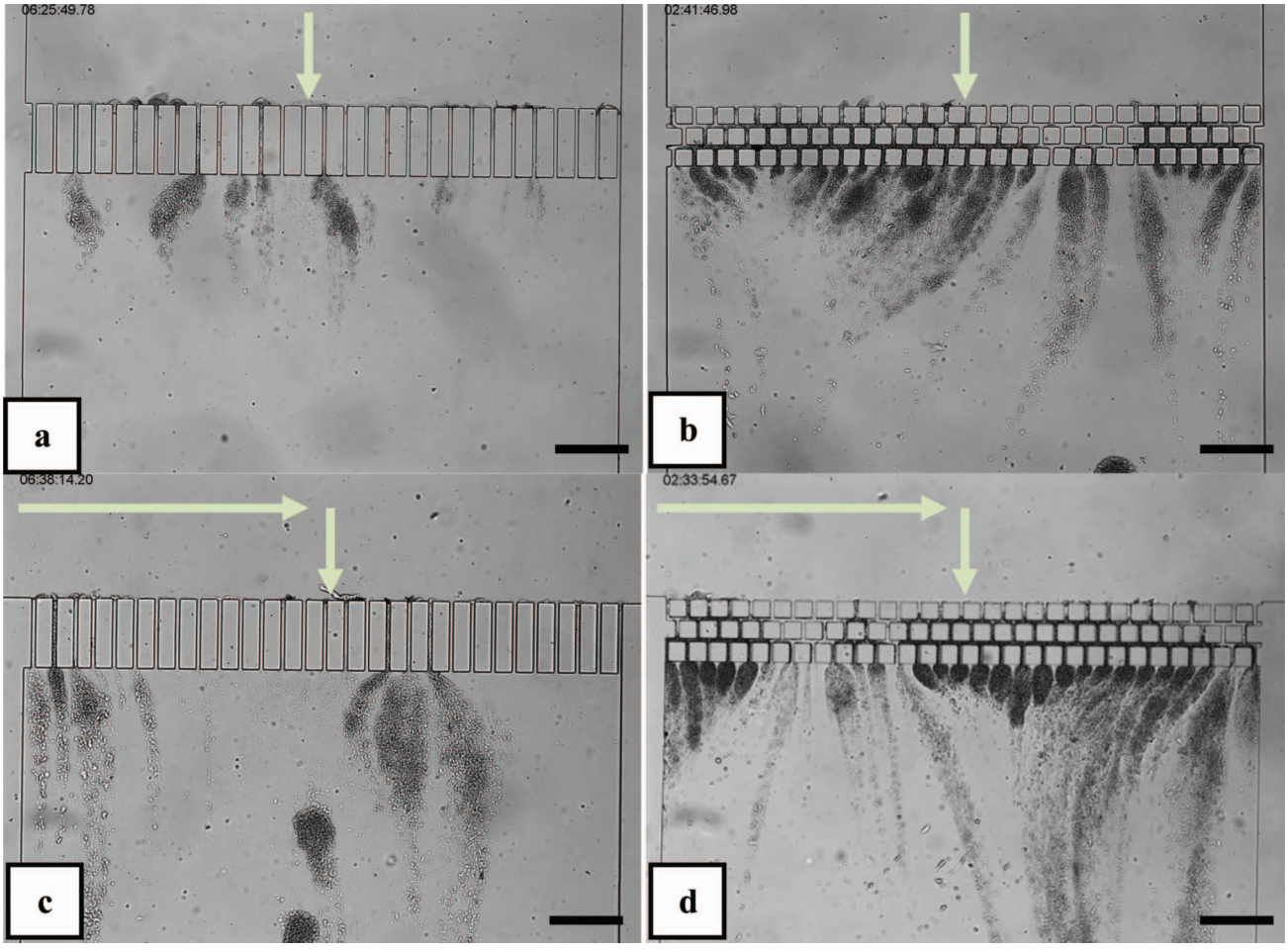

Figure 3. Observation of bacterial development for four different conditions after 2 h filtration. Image a: dead-end mode with straight channels; image b: dead-end mode with staggered channels; image c: pseudo-cross-flow mode with straight channels; image d: pseudo-cross-flow mode with staggered channels. Scale bars = 200 μm.

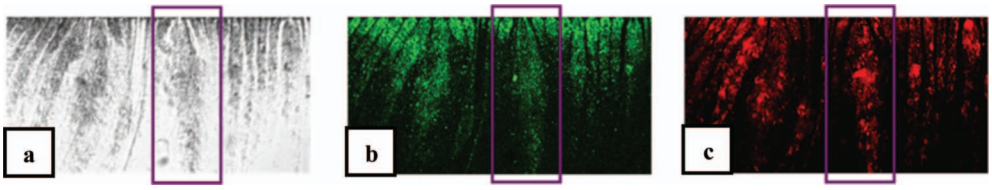

Figure 4. Confocal visualization of a streamer focused at mid-thickness. a: optical image; b: image where bacteria are marked with Syto 9; c: image where EPS is marked with Concanavalin A.

The area of bacteria accumulated is proportional to the picture width and to the average length of streamer growth (l_{av}). The average length is given by the following relationship:

$$l_{av} = \frac{A}{L} \tag{3}$$

where A is the area of accumulated bacteria and L the picture width. It is interesting to plot average streamer length *vs* time to obtain information on the accumulation dynamics.

Experimental results

Accumulation of bacteria was observed for different channel architectures and for channel widths equal to 5, 10, and 20 μm (ie much greater than the size of the bacterial cells). The first part of the section on parametric analysis, below, focuses on the results obtained for 10-μm-wide micro-channels and the effect of channel size is presented for interconnected channels. This size range can be encountered during sand filtration or membrane filtration when the membrane presents abnormally large pores in its structure (Lebleu et al. 2009).

Optical observation of bacterial streamers

Figure 3 shows a micrograph of bacterial accumulation after filtration for 2 h for four configurations with a flow rate of 1.41 ml h^{-1} An unexpected observation, in the xy plane, was that bacteria accumulated after their passage through the microchannels (in the downstream part of the filtering zone). The accumulations will be referred to as 'streamers' because of their specific shape and mobility in the flow, similar to those observed for mature streamers (Stoodley et al. 1998). Even, if in the conditions reported here (non-nutritive and short experimental duration) the streamers were not mature, they could represent the first step in the formation of this kind of biofilm. This result was very different from that observed in same system with 'inert' particles of equivalent size, which were preferentially captured in the bottleneck zone and which then accumulated in the upstream zone (Bacchin et al. 2011).

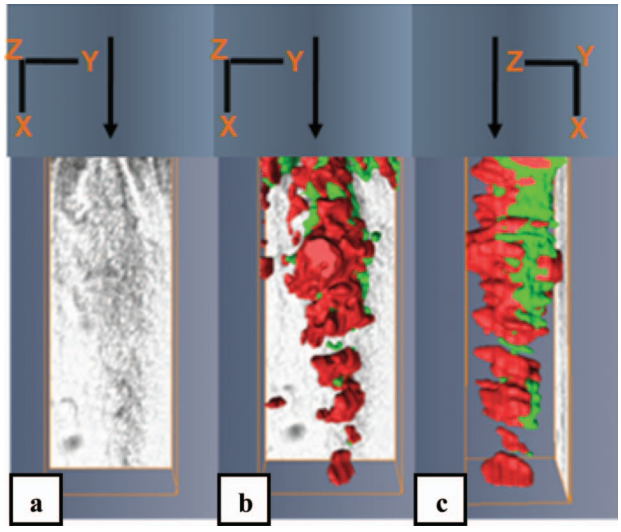

Figure 5. a: Confocal visualization of a streamer in the xy plane; flow is from top to bottom. b and c: three-dimensional reconstruction of a streamer from confocal microscopy in the xy plane (b) and in the xz plane (c); red and green colors represent secreted EPS and bacteria, respectively.

The accumulation also differed when changing the flow conditions. There was almost no accumulation of bacteria when filtering in dead-end mode with straight channels: after filtration for 2 h , only small streamers were observable in the downstream zone (Figure 3a). When experiments were performed with the same channels, but with a pseudo-cross-flow feed, bacterial streamers were observed at the outlet of the channels (Figure 3c). With staggered channels (Figure 3b and d) in both dead-end and pseudo-cross-flow modes, dense streamers occurred.

Confocal microscopy of streamers

Confocal observations were carried out with fluorescent markers to analyze the 3D structure of the streamers and to reveal the presence of the bacteria (green fluorochrome, Figure 4b), and the presence of EPS (red fluorochrome, Figure 4c). Figure 5 shows the reconstruction (Amira software) of the streamers (as selected in Figure 4) obtained after filtration for 120 min.

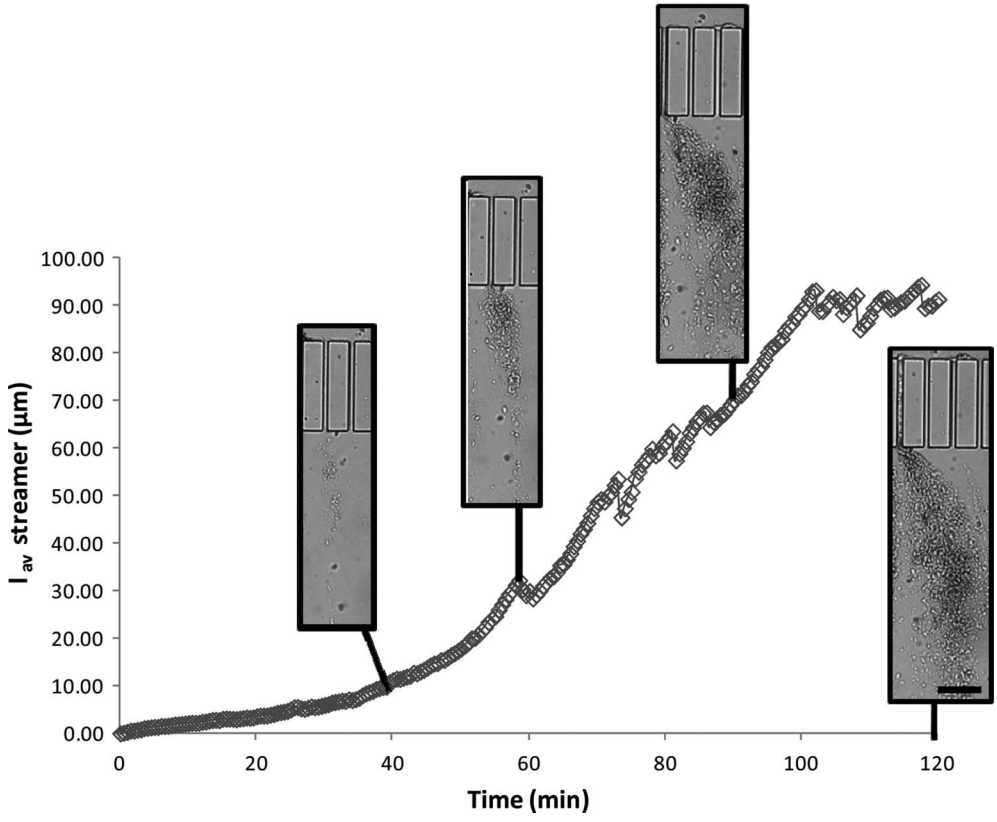

Figure 6. Average streamer length in μm *vs* time for pseudo-cross-flow mode with straight channels. Zoomed images of the downstream zone are given for filtration for 40, 60, 90 and 120 min (Figure 3c). Flow rate: 1.41 ml h^{-1}. Scale bar = 110 μm.

The confocal experiments confirmed the presence of EPS around the bacteria and the presence of the bacteria forming the streamers. The signals for EPS and bacteria are almost superimposed in the images, showing the simultaneous presence of bacteria and EPS at this scale of resolution. It was concluded that the streamers were composed of bacteria with EPS. Streamer reconstruction in the xz plane showed that the streamers spread into the middle of the channel, accounting for the observed undulations in the flow during the filtration experiment (video available in the Supplementary information) [Supplementary material is available *via* a multimedia link on the online article webpage].

Dynamic formation of streamers

The streamers formed progressively during the filtration experiments. To illustrate the dynamics of their formation, Figure 6 shows the area covered by bacterial accumulation *vs* time and in parallel shows zooms of the downstream zone for a given filtration time in the pseudo-cross-flow mode with straight channels. After 40 min, the accumulation of bacteria was observed as tiny filaments having a negligible

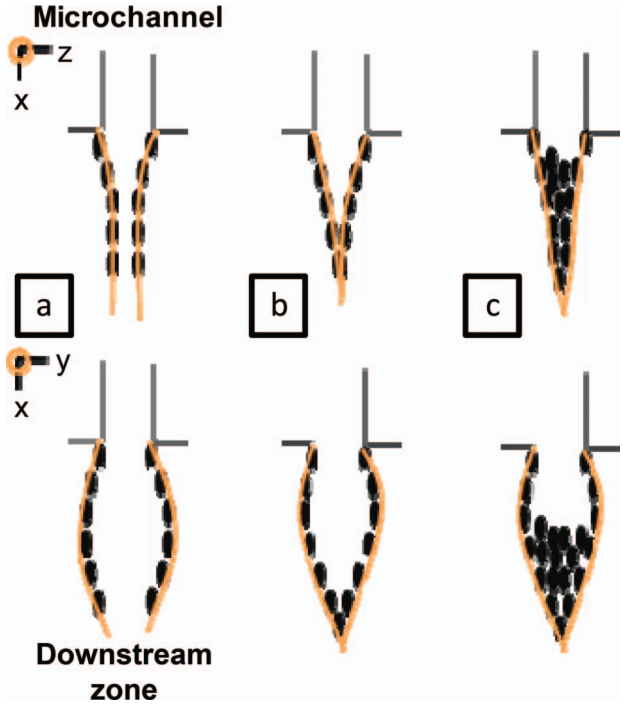

Figure 7. Steps in streamer formation in the xz and xy planes. a: Tiny filaments in the downstream zone; b: filaments join; c: streamers are formed and collect bacteria in a net.

impact on the area of bacterial accumulation. These filaments first adhered to the entrance of the channels on the PDMS wall. After ~1 h, they progressively formed a kind of 'fishing net', by collecting more cells. The net then grows to form a bacterial streamer. By 90 min in these conditions, the streamers grew very rapidly to occupy a large area. The maximum length of the streamers was ~0.5 mm long (containing millions of bacteria), while the mean value was ~0.09 mm (as seen in Figure 6). At later times in the experiment, there was a succession of streamer formation and detachment leading to a rapid decrease in the area of accumulation. The video microscopy (Supplementary material) [Supplementary material is available *via* a multimedia link on the online article webpage] shows that the filaments and the streamers were free to move in the flow and undulated in the stream from a fixed point near the micro-channel outlet. They grew preferentially in the main flow, not in dead-end zones or stagnation points, as might have been expected.

The different steps of streamer formation are represented in Figure 7 in the xz and xy planes. The first step (Figure 7a) was characterized by the presence of tiny filaments. In the second step (Figure 7b) (generally after 1 h), these filaments joined to form the net. Finally, streamers were formed (Figure 7c) by accumulation of bacteria and EPS in the net.

Parametric analysis

The formation of bacterial streamers was analyzed for different flow conditions by varying the channel size, the channel geometries and the flow rate. The growth kinetics of the streamers was quantified by considering their average length (l_{av}) and variation with time. The results were analyzed in terms of capture efficiency corresponding to the ratio of the number of captured bacteria to the number of filtered bacteria in the microseparators.

Effect of channel size

Figures 8 and 9 present the dynamics of bacterial accumulation in the microseparators with connected channels having channel sizes of 5, 10, and 20 μm at a flow rate of 1.41 ml h^{-1}. The velocities in the microchannels were 0.051 m s^{-1}, 0.027 m s^{-1} and 0.016 m s^{-1}, respectively. Figure 8 shows that the average streamer length increased more rapidly as the size of the channel decreased and approached the size of the bacteria (1 × 2 μm). Figure 9 shows data for the capture efficiencies with a picture during filtration for 2 h for the same experiments. From Figures 8 and 9, it can be seen that the formation of streamers was negligible for 20-μm channels, while significant streamers were observed in 5- and 10-μm channels. The width of 20 μm did not seem sufficient to allow the capture of the *E. coli*.

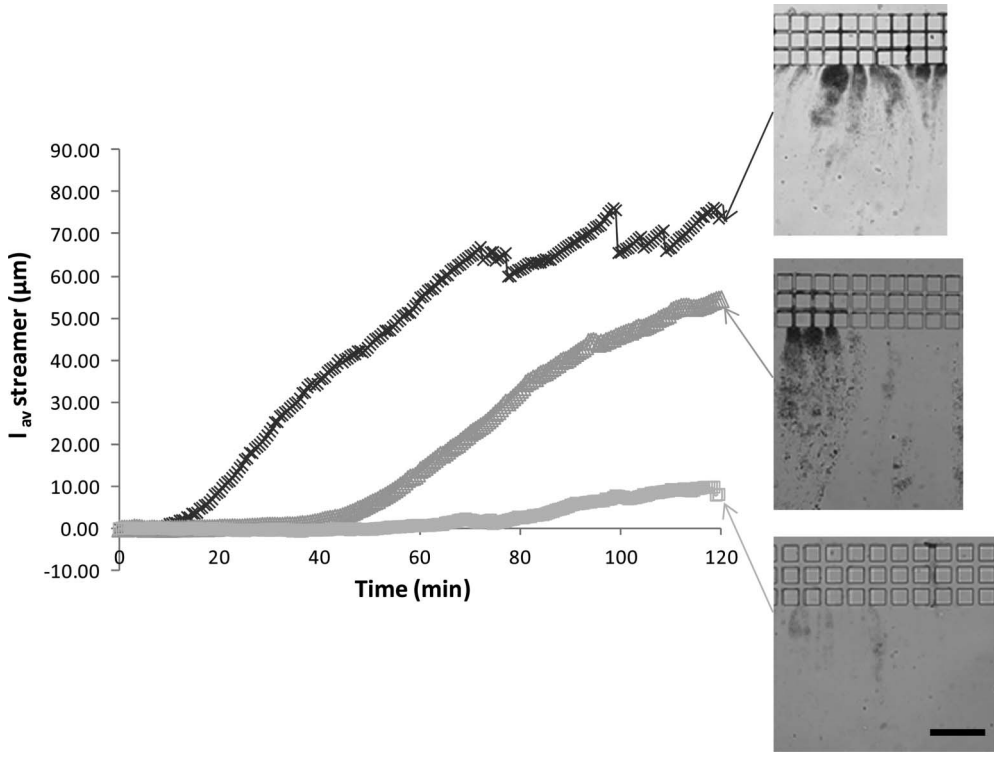

Figure 8. Average streamer length in μm *vs* time for dead-end mode with connected channels and for different channel widths. ×: 5 μm; Δ: 10 μm; □: 20 μm. Scale bar = 170 μm.

Effect of channel connectivity and tortuosity

Figure 10 plots average streamer length against time for dead-end filtration for straight channels, connected channels and staggered row channels having a channel size of 10 μm. It was observed that filtration in staggered rows enhanced streamer formation in the microseparators. By 2 h, the average streamer length was more than twice as long with the staggered than with the straight channels. The difference between connected channels and straight channels was not as great, even though connected channels generally led to a greater capture efficiency.

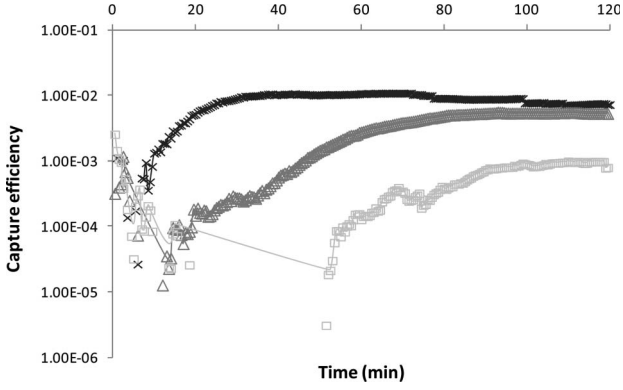

Figure 9. Capture efficiency (number of bacteria caught/number of bacteria passing through the pore) of the microsystem *vs* time for the different channel widths in dead-end mode with connected channels. ×: 5 μm; Δ: 10 μm; □: 20 μm.

Effect of the direction of upstream flow

Figures 11 and 12 compare the dynamics of *E. coli* accumulation in microseparators operating in dead-end or in pseudo-cross-flow filtration modes. The difference in these experiments was the direction of flow in the upstream zone of the microseparators (Figure 3a and 3c). With straight channels, the pseudo-cross-flow configuration led to a slightly greater formation of streamers by the end of the experiments. For the staggered geometry, the final streamer length was almost the same in pseudo-cross-flow and dead-end modes, but a more rapid formation was observed when operating under pseudo-cross-flow. Long streamers only appeared after 25 min with the dead-end configuration, but

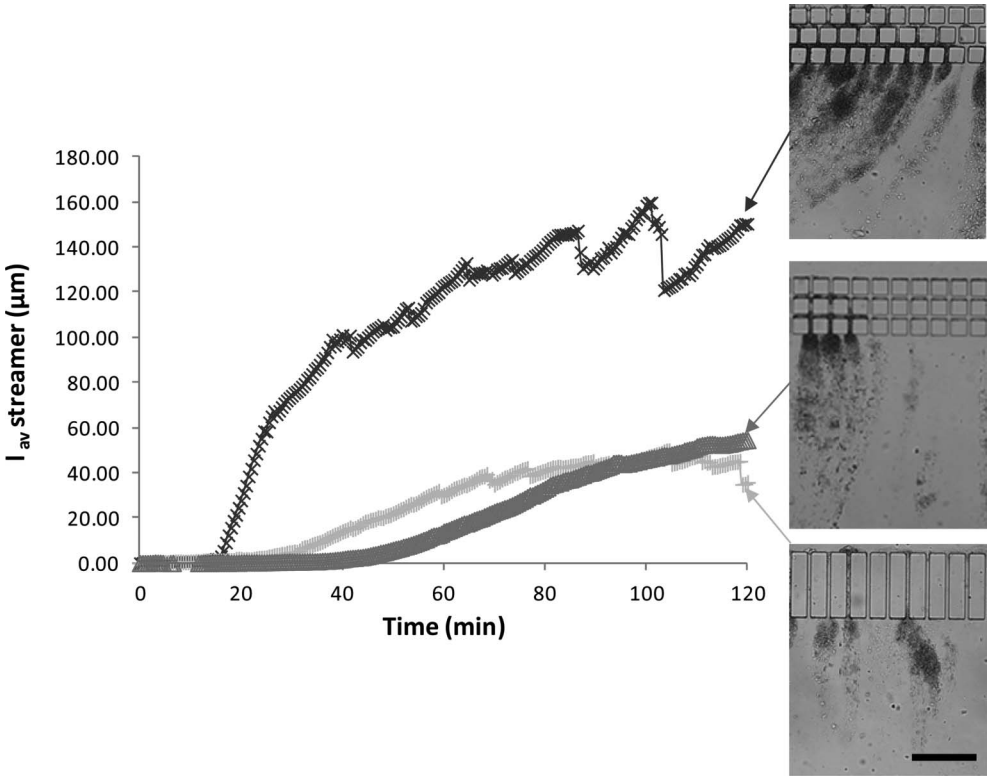

Figure 10. Average streamer length in μm *vs* time for the different 10-μm channel geometries in dead-end mode: ×: staggered channels; Δ: connected channels; +: straight channels. The photographs present the streamers obtained after filtration for 2 h. Scale bar = 170 μm.

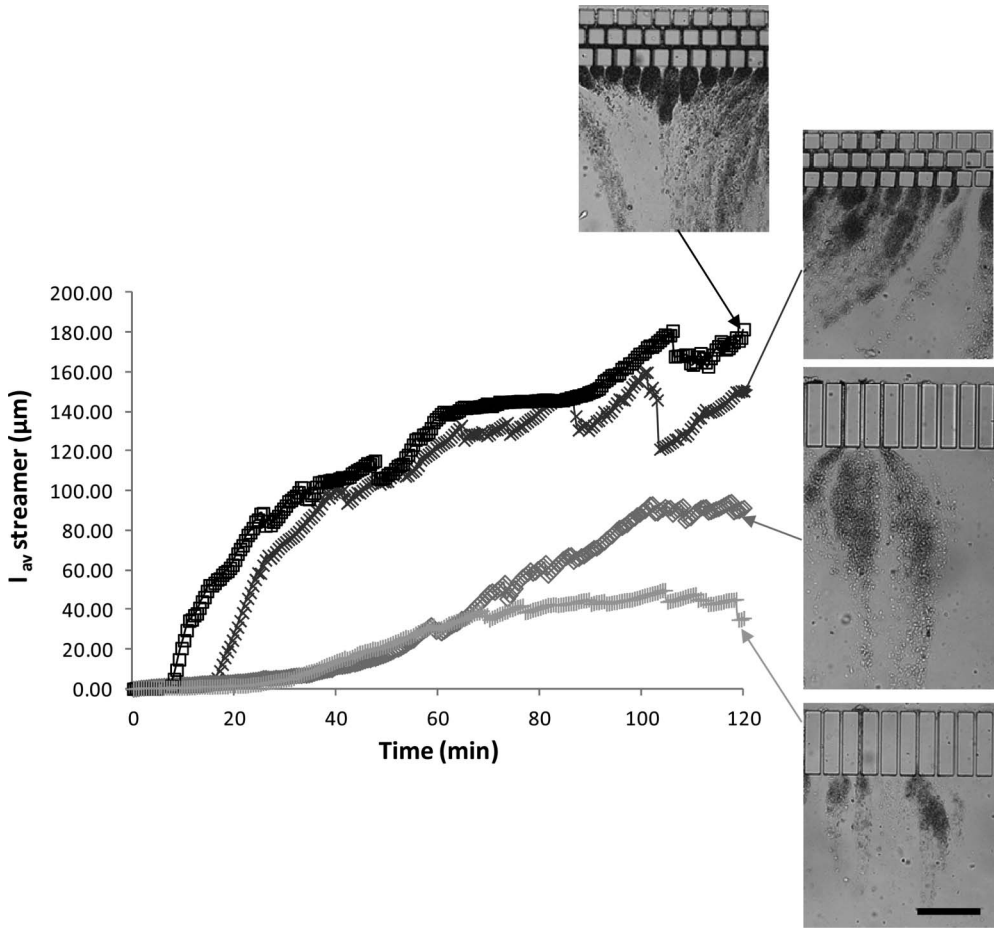

Figure 11. Average streamer length in μm *vs* time for the different flow conditions. ◇: pseudo-cross-flow mode with straight channels; □: pseudo-cross-flow mode with staggered channels; +: dead-end mode with straight channels; ×: dead-end mode with staggered channels. Scale bar = 170 μm.

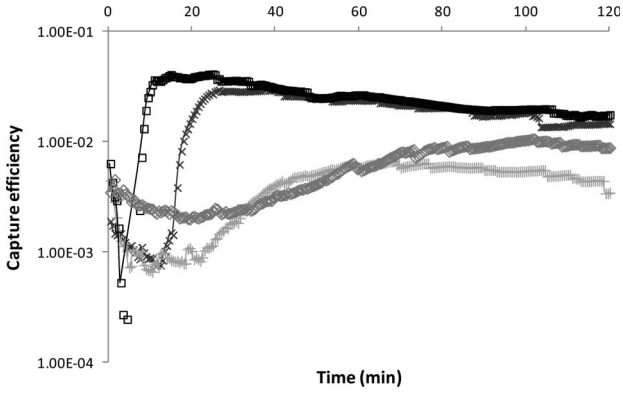

Figure 12. Capture efficiency of the microsystem *vs* time for the different flow conditions. ◇: pseudo-cross flow with straight channels; □: pseudo-cross flow with staggered channels; +: dead-end mode with straight channels; ×: dead-end mode with staggered channels.

were already well formed after 10 min with pseudo-cross-flow. This result indicated that changes in flow direction promoted streamer formation.

Effect of the flow rate

The experiments were performed with different flow rates: 1.41 ml h^{-1}, 7.05 ml h^{-1} and 14.1 ml h^{-1}, corresponding to mean flow velocities in the channels (and Re numbers) of 4.61×10^{-3} m s^{-1} (Re = 0.45), 2.30×10^{-2} m s^{-1} (Re = 2.24) and 4.61×10^{-2} m s^{-1} (Re = 4.48). Figure 13 shows the average streamer length *vs* time for the different flow rates in the dead-end mode with staggered channels. It can be seen that streamer length increased at higher flow rates. Note that, in this range of flow rates, the higher flow velocities did not prevent the formation of streamers. However, the growth of bacterial streamers seemed to reach a limit: no major difference was observed between 7.05 and 14.1 ml h^{-1}. For the highest flow, there were occasional sudden drops in the area of accumulation during the 2-h experiment. These variations were due to the detachment of streamers into the flow. The importance of these phenomena could explain why the growth of the streamers leveled off as the flow rate increased.

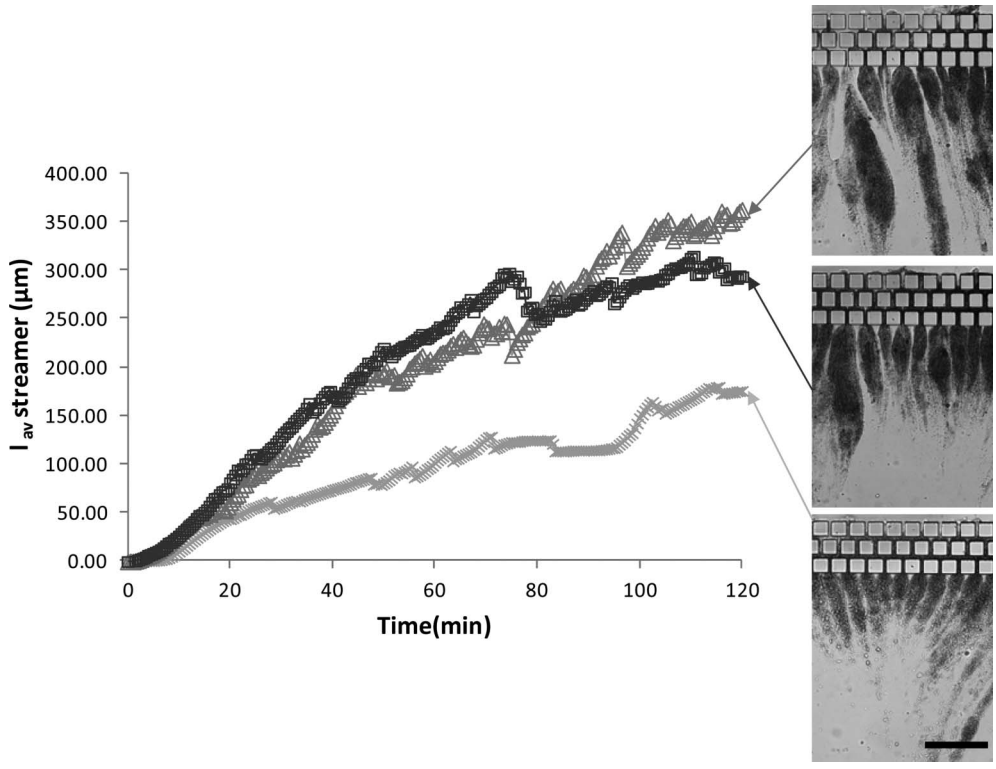

Figure 13. Average streamer length in μm *vs* time for different flow rates in the dead-end mode with staggered channels. $\times$: 1.41 ml h^{-1}; Δ: 7.05 ml h^{-1}; $\square$: 14.1 ml h^{-1}. For each experiment, the photograph was taken after filtration for 2 h. Scale bar = 170 μm.

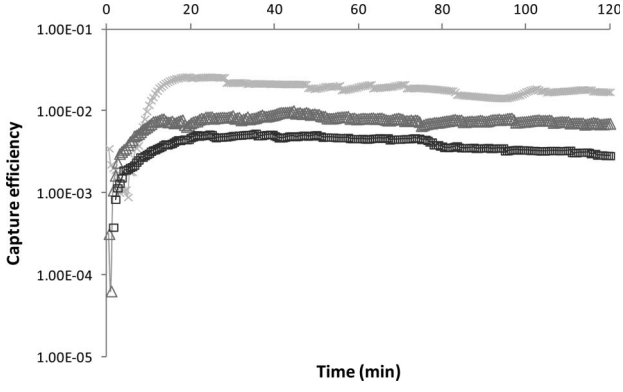

Figure 14. Capture efficiency of microsystem with time for different flow rates for dead-end mode with staggered channels. $\times$: 1.41 ml h^{-1}; Δ: 7.05 ml h^{-1}; $\square$: 14.1 ml h^{-1}.

Unexpectedly, the capture efficiency decreased as the flow rate increased (Figure 14). To understand why the variation in capture efficiency was different from that of the area of accumulation, note that the capture efficiencies account for the bacteria being filtered in the microseparators (in the denominator of the capture efficiency relationship (Equation 2), which increases proportionally with the flow rate. Even though the growth was greater for higher flow rates (Figure 13), the capture efficiency was lower. At higher flow rates, the flux of bacteria through the system was greater, leading to the rapid growth of streamers, but the efficiency of bacterial capture in the streamers was less.

Table 1. Summary of experiments in dead-end mode for different channel architectures (rows) and channel sizes (columns) showing significant bacterial accumulation ($\times$) or negligible bacterial accumulation (o).

	5 μm	10 μm	20 μm
Straight channels	$\times$	$\times$	o
Connected channels	$\times$	$\times$	o
Staggered rows channels	$\times$	$\times$	$\times$

Note: The shaded area corresponds to the experimental conditions presented in the present paper.

Discussion

The experimental results demonstrate the formation of bacterial streamers under different conditions. A wide range of conditions were investigated and data from all are not fully described here. Table 1 summarizes all the experimental conditions, showing which led to significant bacterial accumulation. The filtration of bacteria through the PDMS micro-separators was performed with different channel geometries, channel connectivities and for three channel sizes (5 μm, 10 μm

Table 2. Summary of the effect of different operating parameters on the average streamer length, the formation kinetics and on the capture efficiency.

Operating parameters	Streamer characteristics		
	l_{av}	kinetics	η
Increasing channel size	−	−	−
Increasing channel tortuosity	+	+	+
Change from dead-end mode to pseudo-cross flow mode	+	+	+
Increasing flow rate	+	+	−

Note: (+) the variation of the parameter leads to an increase in streamer characteristics; (−) the variation of the parameter leads to a decrease in streamer characteristics.

and 20 μm). The absence of streamers was noted for larger microchannels (20 μm) or more highly connected channels (ie those not in staggered rows). An important result from these different experiments was that hydrodynamic conditions played an important role in streamer formation.

Table 2 summarizes the effects of different experimental parameters on the average streamer length, the kinetics of streamer formation and the capture efficiency. Small and tortuous channels, low flow rates and the pseudo-cross-flow filtration mode promoted streamer formation; the formation rate and final average length increased. Small channels enhanced bacterial adhesion. The smaller the microchannels, the higher the probability of bacteria-wall collisions. The same was true under the pseudo-cross-flow mode. Once bacteria were caught, it is conceivable that tiny filaments formed, leading to streamer formation.

Under a constant flow rate, the formation of streamers was related to the capture efficiency of the microsystem. When the flow rate was increased, streamer formation was enhanced, but the capture efficiency was reduced; the percentage of flowing bacteria caught by the 'fishing net' was smaller.

In a preliminary study, the results demonstrated that streamer formation and capture efficiency were much more strongly dependent on channel geometry, with a major role played by the tortuosity (due to the use of the staggered geometry) rather than channel connectivity. Higher channel connectivity led to the presence of flow dead zones and stagnation points at each channel connection. These zones did not appear to be as important to streamer formation. On the other hand, changes in the flow direction around corners, as encountered with the staggered geometry, enhanced streamer formation. Such behavior could be related to the presence of secondary flow around corners in microfluidic channels as observed by Rusconi et al. (2010) during their work with streamer formation in *Pseudomonas aeruginosa*.

Conclusions

Direct observations of transfer of *E. coli* through channels (between 5 and 20 μm in size) during filtration in non-nutritive conditions revealed the accumulation of bacteria downstream of the filter. During filtration, *E. coli* accumulation took the form of tiny filaments that progressively joined to form a net collecting cells which grew to form a streamer of bacteria. When filtering *E. coli* in 5- and 10-μm channels, the bacteria formed streamers that were approximately 200 μm long in the downstream zone. In contrast, with 20-μm channels, the formation of streamers was negligible.

Confocal microscopy and 3D reconstruction of streamers showed that the streamers were connected to the filter, but free to move in the stream. The use of specific markers confirmed that the streamers were composed of cells and exopolysaccharide. Streamers occurred in high-flow zones. The presence of a dead-end zone in the flow (in connected channels) did not promote the formation of streamers. In contrast, the tortuosity of the porous zone (staggered) led to the formation of streamers that were larger and that grew more rapidly. The streamers grew slightly faster when the micro-separators worked in a pseudo-cross-flow mode.

This work shows that filtering bacteria through pores larger than the bacterial cells (ie not retentive of bacteria) can lead to an accumulation of bacteria and EPS in the downstream area of the filter. The formation of streamers could have important consequences in filtration processes involving bacterial suspensions (eg sand filtration and prefiltration operations), such as those be found in drinking water production. The streamers represent a possible source of recurrent contamination. Further investigations should be performed to establish the relationship between the formation of these streamers and the hydrodynamic and biological conditions.

Acknowledgements

The authors thank William Mark Durham, Roberto Rusconi and Howard Stone for helpful discussions. They also acknowledge Paul Duru (IMFT) for scientific help, David Bourrier (RTB-LAAS) for technical support in making the micro-separators and the 'FERMAT Federation' (FR CNRS 3089) for partly funding this research work. Cecile Pouzet from INRA (IFR40) is thanked for providing the confocal microscopy images.

References

Abbasnezhad H, Gray MR, Foght JM. 2008. Two different mechanisms for adhesion of Gram-negative bacterium, *Pseudomonas fluorescens* LP6a, to an oil-water interface. Colloids Surf B: Biointerfaces 62:36–41.

Bacchin P, Marty A, Duru P, Meireles M, Aimar P. 2010. Colloidal surface interactions and membrane fouling: investigations at pore scale. Adv Colloid Interfac 164:2–11.

Bruinsma GM, Rustema-Abbing M, Van der Mei HC, Busscher H J. 2001. Effects of cell surface damage on surface properties and adhesion of *Pseudomonas aeruginosa*. Microbiol Meth 45:95–101.

Burks GA, Velegol SB, Paramonova E, Lindenmuth BE, Feick JD, Logan BE. 2003. Macroscopic and nanoscale measurements of adhesion of bacteria with varying outer layer surface composition. Langmuir 19:2366–2371.

Chu HP, Li X. 2005. Membrane fouling in a membrane bioreactor (MBR): sludge cake formation and fouling characteristics. Biotechnol Bioeng 90:323–331.

de Kerchove AJ, Elimelech M. 2008. Bacterial swimming motility enhances cell deposition and surface coverage. Environ Sci Technol 42:4371–4377.

de La Fuente L, Montanes E, Meng Y, Li Y, Burr TJ, Hoch HC, Wu M. 2007. Assessing adhesion forces of type I and IV pili of *Xylella fastidiosa* bacteria using a microfluidic chamber. Appl Environ Microbiol 73:2690–2696.

Gaboriaud F, Gee ML, Strugnell R, Duval JFL. 2008. Coupled electrostatic, hydrodynamic, and mechanical properties of bacterial interfaces in aqueous media. Langmuir 24:10988–10995.

Gannon JT, Manilal VB, Alexander M. 1991. Relationship between cell-surface properties and transport of bacteria through soil. Appl Environ Microbiol 57:190–193.

Jewett DG, Hilbert TA, Logan BE, Arnold RG, Bales RC. 1995. Bacterial transport in laboratory columns and filters: influence of ionic strength and pH on collision efficiency. Water Res 29:1673–1680.

Lebleu N, Roques C, Aimar P, Causserand C. 2009. Role of the cell-wall structure in the retention of bacteria by microfiltration membranes. J Membrane Sci 326:178–185.

Li X, Chu HP. 2003. Membrane bioreactor for the drinking water treatment of polluted surface water supplies. Water Res 37:4781–4791.

Liu Y, Li J. 2008. Role of *Pseudomonas aeruginosa* biofilm in the initial adhesion, growth and detachment of *Escherichia coli* in porous media. Environ Sci Technol 42:443–449.

McDonald JC, Duffy DC, Anderson JR, Chiu DT, Wu H, Schueller OJA, Whitesides GM. 2000. Fabrication of microfluidic systems in poly(dimethylsiloxane). Electrophoresis 21:27–40.

Redman JA, Walker SL, Elimelech M. 2004. Bacterial adhesion and transport in porous media: role of the secondary energy minimum. Environ Sci Technol 38. 1777–1785.

Rusconi R, Lecuyer S, Guglielmini L, Stone HA. 2010. Laminar flow around corners triggers the formation of biofilm streamers. J R Soc Interface 7:1293–1299.

Schäfer A, Harms H, Zehnder AJB. 1998. Bacterial accumulation at the air-water interface. Environ Sci Technol 32:3704–3712.

Stephenson T, Brindle K, Judd S, Jefferson B. 2000. Membrane bioreactors for wastewater treatment. London (UK): IWA Publishing. p. 59–61.

Stoodley P, Lewandowski Z, Boyle JD, Lappin-Scott HM. 1998. Oscillation characteristics of biofilm streamers in turbulent flowing water as related to drag and pressure drop. Biotechnol Bioeng 57:536–544.

Torkzaban S, Tazehkand SS, Walker SL, Bradford SA. 2008. Transport and fate of bacteria in porous media: coupled effects of chemical conditions and pore space geometry. Water Res 44:1–12.

Ueshima M, Ginn BR, Haack EA, Szymanowski JES, Fein JB. 2008. Cd adsorption onto *Pseudomonas putida* in the presence and absence of extracellular polymeric substance. Geochim Cosmochim Acta 72:5885–5895.

Van Loosdrecht MC, Lyklema J, Norde W, Schraa G, Zehnder AJ. 1987. The role of bacterial-cell wall hydrophobicity in adhesion. Appl Environ Microbiol 53:1893–1897.

Vrouwenvelder JS, Graf von der Schulenburg DA, Kruithof JC, Johns ML, van Loosdrecht MCM. 2009. Biofouling of spiral-wound nanofiltration and reverse osmosis membranes : a feed spacer problem. Water Res 43:583–594.

Walker SL, Redman JA, Elimelech M. 2004. Role of cell surface lipopolysaccharides in *Escherichia coli* K12 adhesion and transport. Langmuir 20:7736–7746.